Radio Science, Volume 29, Number 4, Pages 1101–1118, July–August 1994

Simultaneous nonlinear reconstruction of two-dimensional permittivity and conductivity

Tarek M. Habashy and Michael L. Oristaglio
Schlumberger-Doll Research, Ridgefield, Connecticut

Adrianus T. de Hoop
Delft University of Technology, Department of Electrical Engineering, Delft, Netherlands

Abstract. A new inversion algorithm for the simultaneous reconstruction of permittivity and conductivity recasts the nonlinear inversion as the solution of a coupled set of linear equations. The algorithm is iterative and proceeds through the minimization of two cost functions. At the initial step the data are matched through the reconstruction of the radiating or minimum norm scattering currents; subsequent steps refine the nonradiating scattering currents and the material properties inside the scatterer. Two types of basis functions are constructed for the nonradiating currents: "invisible" (global) basis functions, which are appropriate for discrete measurements and nonradiating (local) basis functions, which are useful in studying the limit of continuous measurements. Reconstructions of square cylinders from multiple source receiver measurements at a single frequency show that the method can handle large contrasts in material properties.

1. Introduction

Most practical algorithms for inverse scattering assume that the scatterer is a small perturbation of a known background medium. Included in this category are the ordinary and distorted wave Born approximations, either when used in a single, linear imaging step or in an iterative, nonlinear search for the best model [*Habashy and Mittra*, 1987]. Perturbative methods have difficulty when the perturbation is large, that is, when the scatterer is large in size or when its material properties differ from those of the known medium by a large amount [e.g., *Kleinman and van den Berg*, 1990a, b].

This paper describes some improvements in an inverse scattering algorithm that we call the source type integral equation or STIE method [*Habashy et al.*, 1992; *Caorsi et al.*, 1992, 1991, 1990; *Bolomey et al.*, 1991; *Ney et al.*, 1984]. These improvements attempt to deal with large perturbations in material properties. We will describe the method for a multiparameter inverse problem in scalar electromagnetic scattering, but it applies to any scattering problem governed by the scalar or vector Helmholtz equation. In any scattering problem, both the field measured outside the scatterer (the data) and the (unknown) field inside the scatterer can be related by a linear integral equation to equivalent sources in the scatterer. In electromagnetics the equivalent sources are usually called scattering currents. The scattering currents are, in turn, linearly related by a constitutive equation to the field inside the scatterer and the difference in material properties between the scatterer and an arbitrary background medium. The STIE method tries to solve the nonlinear inverse scattering problem for the material properties by inverting these two linear relations (the global integral equation between the field and its sources and the local constitutive relation between the sources and the material properties) in two separate steps.

To motivate this approach, consider first a naive application of the method. In the naive STIE method the integral equation between the field and the scattering currents is inverted to obtain the scattering currents from the data (the field outside the scatterer). This first step involves the solution of a linear inverse source problem. Next, the field inside the scatterer is computed using the scattering currents obtained from the first step. This second step is just the linear computation of a field given its sources. Finally, the scattering currents are divided

Paper number 93RS03448.
0048-6604/94/93RS-03448$08.00

by the field computed inside the scatterer to give the material properties. In principle, this procedure solves the nonlinear inverse scattering problem by direct linear methods, without assuming that the contrast in material properties is small.

Obviously, the naive STIE method cannot always work perfectly. It is defeated by the nonuniqueness of the inverse source problem that must be solved to obtain the scattering currents from the data. Inverse source problems are nonunique because of nonradiating sources [*Devaney and Wolf*, 1973; *Bleistein and Cohen*, 1977]. In electromagnetics, nonradiating sources are currents that generate zero electric and magnetic field outside their domain of support. If the currents induced in a scattering experiment include any nonradiating currents, then the data contain no information about these currents, and it is therefore impossible, without other information, to reconstruct the full scattering currents and the full field inside the scatterer with a linear inversion. Moreover, this nonuniqueness cannot be overcome by simply adding more experiments (different incident fields and frequencies) because the induced scattering currents change with the incident field and the frequency. Each new experiment increases the nonuniqueness rather than reducing it.

Nevertheless, it is known that inverse scattering problems with multiple experiments can have unique solutions [*Devaney and Sherman*, 1982]. The reason is that, although the scattering currents change with each experiment, the unknown material properties do not change (the material properties of a linear medium do not depend on the incident field, and often their frequency dependence can be given a simple explicit form). The combination of different incident fields or different frequencies makes the inversion for the material properties a well-posed, but nonlinear, problem. The naive STIE method must be modified ("renormalized") to incorporate this feature [*Habashy et al.*, 1990; *Habashy and Dudley*, 1989a, b]. The resulting algorithm is iterative but appears to be computationally efficient for large perturbations. An important part of the STIE method described here is the construction and use of explicit basis functions for the nonradiating currents. Although these currents contribute nothing to the data, they are needed to maintain the field inside the scatterer consistent with its material properties. In fact, with the STIE method the data is inverted only once for the radiating currents; subsequent iterations refine just the nonradiating currents.

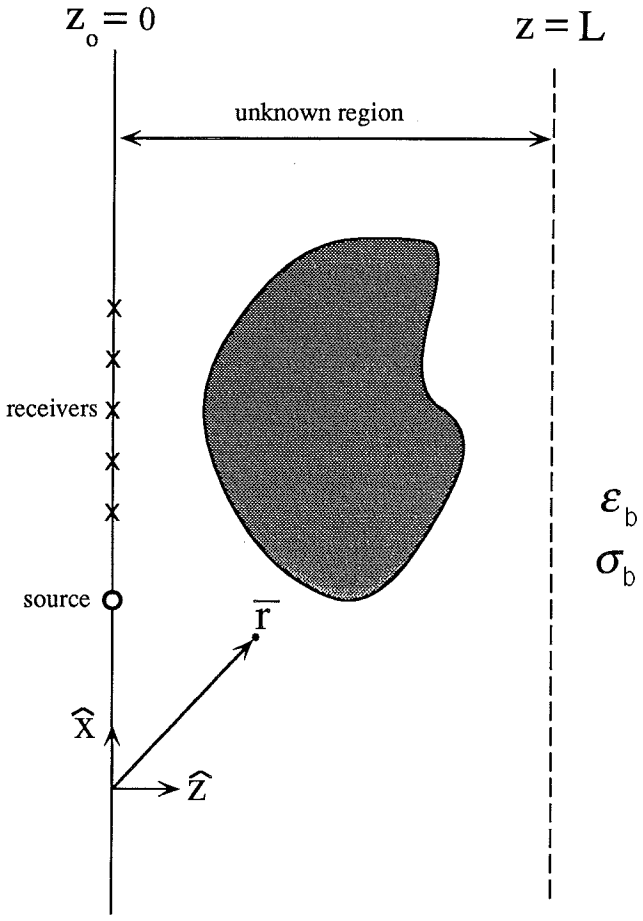

Figure 1. Schematic of the inversion problem.

2. Basic Equations

Figure 1 shows the two-dimensional (2-D) geometry that we will use to illustrate the STIE method. The position vector in the 2-D plane will be denoted by $\bar{r} = x\hat{x} + z\hat{z}$. We limit ourselves to the transverse electric (TE) polarization with an electric line current source of unit strength, situated at $\bar{r}_n = x_n\hat{x} + z_n\hat{z}$ ($z_n \leq 0$) and extending from $y = -\infty$ to $y = +\infty$. The nonzero field components are then H_x, H_z, and E_y, which are functions of x and z only. We assume an exp $(-i\omega t)$ time dependence for these fields, where ω is the (angular) frequency.

The governing equation for the electric field $E \equiv E_y$ is then

$$\nabla^2 E(\bar{r}, \bar{r}_n) + k^2(\bar{r})E(\bar{r}, \bar{r}_n) = -i\omega\mu_0 J(\bar{r}, \bar{r}_n),$$

where $J(\bar{r}, \bar{r}_n) = \delta(\bar{r} - \bar{r}_n)$ is the impressed current,

$$k^2(\bar{r}) = \omega^2 \mu_0 \varepsilon(\bar{r}) + i\omega\mu_0\sigma(\bar{r}),$$

$\varepsilon(\bar{r})$ is the electrical permittivity, $\sigma(\bar{r})$ is the electrical conductivity, and μ_0 is the electrical permeability (assumed to be constant). To develop the basic equations further, we assume that the medium consists of a homogeneous background with known permittivity ε_b and conductivity σ_b, in which is embedded an unknown region which extends from $z = 0$ to $z = L$. The unknown region includes the scatterer but is not necessarily limited to it. We also assume that measurements are available continuously along the line $z_0 = 0$ from $x = -\infty$ to $x = +\infty$. Appendix A shows how to develop the equations for discretely sampled fields.

The electric field can be split into a background field E_b and a scattered field E_s,

$$E(\bar{r}, \bar{r}_n) = E_b(\bar{r}, \bar{r}_n) + E_s(\bar{r}, \bar{r}_n). \tag{1}$$

The equations for E_b and E_s are

$$\nabla^2 E_b(\bar{r}, \bar{r}_n) + k_b^2 E_b(\bar{r}, \bar{r}_n) = -i\omega\mu_0 J(\bar{r}, \bar{r}_n), \tag{2}$$

$$\nabla^2 E_s(\bar{r}, \bar{r}_n) + k_b^2 E_s(\bar{r}, \bar{r}_n) = -i\omega\mu_0 J_s(\bar{r}, \bar{r}_n), \tag{3}$$

where

$$k_b^2 = \omega^2\mu_0\varepsilon_b + i\omega\mu_0\sigma_b \tag{4}$$

and $J_s(\bar{r}, \bar{r}_n)$ is the scattering current,

$$J_s(\bar{r}, \bar{r}_n) = Q(\bar{r})E(\bar{r}, \bar{r}_n), \tag{5}$$

with

$$Q(\bar{r}) = [\sigma(\bar{r}) - \sigma_b] - i\omega[\varepsilon(\bar{r}) - \varepsilon_b]. \tag{6}$$

$Q(\bar{r})$ is the unknown to be determined and is related to the difference in the electrical properties $\varepsilon(\bar{r})$ and $\sigma(\bar{r})$ between the inhomogeneous region and the background.

Equations (1)–(3) are equivalent to the integral equation [*Kong*, 1986]

$$E(\bar{r}, \bar{r}_n) = E_b(\bar{r}, \bar{r}_n) + \int_0^L dz' \int_{-\infty}^{\infty} dx'\, g(\bar{r}, \bar{r}')J_s(\bar{r}', \bar{r}_n), \tag{7}$$

or

$$E_s(\bar{r}, \bar{r}_n) = \int_0^L dz' \int_{-\infty}^{\infty} dx'\, g(\bar{r}, \bar{r}')J_s(\bar{r}', \bar{r}_n), \tag{8}$$

where $g(\bar{r}, \bar{r}')$ is the two-dimensional Green function,

$$g(\bar{r}, \bar{r}') = -\frac{\omega\mu_0}{4} H_0^{(1)}(k_b|\bar{r} - \bar{r}'|), \tag{9}$$

which satisfies

$$\nabla^2 g(\bar{r}, \bar{r}') + k_b^2 g(\bar{r}, \bar{r}') = -i\omega\mu_0\delta(\bar{r} - \bar{r}'). \tag{10}$$

and $E_b(\bar{r}, \bar{r}_n) = g(\bar{r}, \bar{r}_n)$. Equations (5) and (7) are the basic equations of the STIE method. Equation (7) (or (8)) is the global integral relation between the field and the scattering currents, whereas (5) is the local constitutive relation between these two quantities and the material properties. Equation (8) applies whether the observation point $\bar{r}$ is inside or outside the scatterer and will be used in two ways: first, as an integral equation to be solved for J_s given the field E_s measured outside the scatterer, and second, to compute the field E inside the scatterer given an estimate for J_s.

In the geometry of Figure 1, the above equations can be reduced to one-dimensional equations, often having explicit solutions, by a Fourier transformation along the x direction:

$$\tilde{E}(k_x, z, \bar{r}_n) = \tilde{E}_b(k_x, z, \bar{r}_n) + \int_0^L dz'\, G(k_x, z, z')\tilde{J}_s(k_x, z', \bar{r}_n), \tag{11}$$

where

$$\tilde{E}_b(k_x, z, \bar{r}_n) = G(k_x, z, z_n)e^{-ik_x x_n}, \tag{12}$$

$$\tilde{E}(k_x, z, \bar{r}_n) = \frac{1}{2\pi}\int_{-\infty}^{\infty} dx\, e^{-ik_x x}E(\bar{r}, \bar{r}_n), \tag{13}$$

$$\tilde{J}_s(k_x, z, \bar{r}_n) = \frac{1}{2\pi}\int_{-\infty}^{\infty} dx\, e^{-ik_x x}J_s(\bar{r}, \bar{r}_n). \tag{14}$$

$G(k_x, z, z')$ is now the one-dimensional Green function,

$$G(k_x, z, z') = -\frac{\omega\mu_0}{2k_{bz}} e^{ik_{bz}|z - z'|}, \tag{15}$$

which satisfies

$$\left[\frac{d^2}{dz^2} + k_{bz}^2\right]G(k_x, z, z') = -i\omega\mu_0\delta(z - z'), \tag{16}$$

where

$$k_{bz}^2 = k_b^2 - k_x^2. \tag{17}$$

In general, k_{bz} is complex,

$$k_{bz} = k'_{bz} + ik''_{bz}, \tag{18}$$

with $k'_{bz} = \text{Re}\{k_{bz}\}$ and $k''_{bz} = \text{Im}\{k_{bz}\} \geq 0$. For any k_x, (11) corresponds to an excitation by a plane wave whose wavenumber has the components k_x along the x axis and k_{bz} along the z axis.

3. Inverse Source and Scattering Problems

When coupled in the inverse scattering problem, by substituting (5) into (7), these basic equations become a single nonlinear equation for Q, because the total field E inside the scatterer, which multiplies Q, is unknown and depends on Q. The STIE method keeps these equations separate and treats the nonlinear inverse scattering problem in two steps. The first step is the inversion of (8) for the induced scattering currents J_s using the fields measured outside the scatterer. The direct inversion for J_s is a linear inverse source problem. The second step is the calculation of a consistent electric field E and material properties Q inside the scatterer. This section describes the solution of the inverse source problem.

Inversion for $J_s(\bar{r}, \bar{r}_n)$ is conveniently done in the k_x domain with (11), rewritten to relate the scattered field along the measurement line z_0 to the scattering currents,

$$\int_0^L dz'\, G(k_x, z_0, z')\tilde{J}_s(k_x, z', \bar{r}_n) = \tilde{E}_s(k_x, z_0, \bar{r}_n). \tag{19}$$

The scattered field recorded along the line z_0,

$$\tilde{E}_s(k_x, z_0, \bar{r}_n) = \tilde{E}(k_x, z_0, \bar{r}_n) - \tilde{E}_b(k_x, z_0, \bar{r}_n), \tag{20}$$

will be called the data. Equation (19), which is an integral equation of the first kind for the z dependence of $\tilde{J}_s$ (at each k_x and each source position $\bar{r}_n$), does not have a unique solution. The nonuniqueness is easily shown by substituting for $\tilde{J}_s$ a function of the form

$$\tilde{J}_R(k_x, z, \bar{r}_n) = j(k_x, \bar{r}_n) f(k_x, z, \bar{r}_n), \tag{21}$$

and rearranging, which gives

$$j(k_x, \bar{r}_n) = \frac{1}{F(k_x, \bar{r}_n)} \tilde{E}_s(k_x, z_0, \bar{r}_n), \tag{22}$$

provided

$$F(k_x, \bar{r}_n) = \int_0^L dz'\, G(k_x, z_0, z') f(k_x, z', \bar{r}_n) \tag{23}$$

is not zero. Thus the function

$$\tilde{J}_R(k_x, z, \bar{r}_n) = \frac{\tilde{E}_s(k_x, z_0, \bar{r}_n)}{F(k_x, \bar{r}_n)} f(k_x, z, \bar{r}_n) \tag{24}$$

solves (19). Obviously, there are infinitely many of these solutions, and because the equation is linear the difference of any two of them is a current distribution that gives zero field along the measurement line z_0. We call such a current distribution nonradiating and denote it by $\tilde{J}_{NR}$; it satisfies

$$\int_0^L dz'\, G(k_x, z_0, z')\tilde{J}_{NR}(k_x, z', \bar{r}_n) = 0. \tag{25}$$

The set of all solutions to eq. (25) is called the annihilator of the kernel $G(k_x, z_0, z')$. Clearly, an arbitrary linear combination of elements in the annihilator can be added to any particular solution of (19), and the result will still satisfy (19). Thus the data $\tilde{E}_s(k_x, z_0, \bar{r}_n)$ contain no information about the part of the induced current distribution $\tilde{J}_s$ that belongs to the annihilator.

A particular solution of (19) can be constructed by imposing additional conditions. An example is the solution that has the smallest L_2 norm,

$$\|\tilde{J}_s(k_x, z, \bar{r}_n)\|^2 \equiv \langle \tilde{J}_s(k_x, z, \bar{r}_n), \tilde{J}_s(k_x, z, \bar{r}_n) \rangle$$

$$= \int_0^L dz\, |\tilde{J}_s(k_x, z, \bar{r}_n)|^2.$$

This minimum norm solution is obtained by setting

$$f(k_x, z', \bar{r}_n) = G^*(k_x, z_0, z'), \tag{26}$$

in (24), where the asterisk denotes complex conjugation. The minimum norm solution is thus

$$\tilde{J}_{MN}(k_x, z', \bar{r}_n) = \frac{\tilde{E}_s(k_x, z_0, \bar{r}_n)}{N^2(k_x)} G^*(k_x, z_0, z'), \tag{27}$$

where

$$N^2(k_x) = \int_0^L dz'' \, |G(k_x, z_0, z'')|^2. \tag{28}$$

In the spatial domain,

$$J_{MN}(\bar{r}', \bar{r}_n) = \int_{-\infty}^{\infty} dk_x \, e^{ik_x x'} \frac{1}{N^2(k_x)} \cdot G^*(k_x, z_0, z') \tilde{E}_s(k_x, z_0, \bar{r}_n), \tag{29}$$

which becomes a convolutional integral,

$$J_{MN}(\bar{r}, \bar{r}_n) = \int_{-\infty}^{\infty} dx' \, \Gamma(x - x', z) E_s(x', z_0, \bar{r}_n), \tag{30}$$

where $\Gamma(x - x', z)$ is the "pseudoinverse" of $g(x, z_0, \bar{r}')$ given by

$$\Gamma(x', z') = \frac{1}{2\pi} \int_{-\infty}^{\infty} dk_x \, e^{ik_x x'} \frac{1}{N^2(k_x)} G^*(k_x, z_0, z'). \tag{31}$$

Equation (29) for J_{MN} can be interpreted as the backpropagation of the scattered field (weighted or filtered by $1/N^2$) from the measurement line z_0 into the background medium. Appendix B discusses other properties of the minimum norm currents and their relationship to the actual induced currents.

The minimum norm solution of (29) is an expansion of the scattering currents $\bar{J}_{MN}$ in the basis functions $G^*(k_x, z_0 = 0, z)$ (which are indexed by k_x). These basis functions can not, in general, represent fully the actual scattering currents. The scattering currents will usually have a nonradiating part $\bar{J}_{NR}$, which must be included to solve the original inverse scattering problem. Thus the general solution of (19) is a linear combination of the minimum norm solution and an arbitrary nonradiating source,

$$\bar{J}_s(k_x, z, \bar{r}_n) = \bar{J}_{MN}(k_x, z, \bar{r}_n) + \bar{J}_{NR}(k_x, z, \bar{r}_n), \tag{32}$$

where $\bar{J}_{NR}(k_x, z, \bar{r}_n)$ is a weighted superposition of the solutions to (25). The L_2 norm of this general solution is

$$\|\bar{J}_s(k_x, z, \bar{r}_n)\|^2 = \|\bar{J}_{MN}(k_x, z, \bar{r}_n)\|^2 + \|\bar{J}_{NR}(k_x, z, \bar{r}_n)\|^2, \tag{33}$$

which follows because $\bar{J}_{MN}$ is orthogonal to any nonradiating source; indeed,

$$\int_0^L dz' \, \bar{J}^*_{MN}(k_x, z', \bar{r}_n) \bar{J}_{NR}(k_x, z', \bar{r}_n) = \frac{\tilde{E}^*_s(k_x, z_0, \bar{r}_n)}{N^2(k_x)} \cdot \int_0^L dz' \, G(k_x, z_0, z') \bar{J}_{NR}(k_x, z', \bar{r}_n) \equiv 0. \tag{34}$$

Equation (33) shows explicitly that J_{MN} is the solution of (19) with the smallest L_2 norm and excludes all elements of the annihilator.

According to (29), the minimum norm part of the general solution is uniquely determined by the data. The nonradiating part will have to be fixed by considerations beyond the inversion of (19). This will be discussed in the next sections.

4. Electric Field Inside the Scatterer

The second step in the STIE method is the determination, inside the scatterer, of an electric field and material properties that are consistent with the incident field and the minimum norm scattering currents obtained by inverting the data. Equation (11) and the results of the previous section show that the electric field inside the scatterer should be split into three terms: the background or incident field E_b, the field generated by the minimum norm scattering currents E_{MN}, and the field generated by the nonradiating scattering currents E_{NR}:

$$\bar{E}(k_x, z, \bar{r}_n) = \bar{E}_b(k_x, z, \bar{r}_n) + \bar{E}_{MN}(k_x, z, \bar{r}_n) + \bar{E}_{NR}(k_x, z, \bar{r}_n). \tag{35}$$

Note that E_{NR}, the electric field of the nonradiating scattering currents, will be nonzero inside the scatterer. Each of these electric fields can be computed by operating on their current distributions with the Green function; specifically, for E_{NR} and E_{MN},

$$\bar{E}_{NR}(k_x, z, \bar{r}_n) = \int_0^L dz' \, G(k_x, z, z') \bar{J}_{NR}(k_x, z', \bar{r}_n), \tag{36}$$

$$\bar{E}_{MN}(k_x, z, \bar{r}_n) = \int_0^L dz' \, G(k_x, z, z') \bar{J}_{MN}(k_x, z', \bar{r}_n) = \frac{\bar{E}_s(k_x, z_0, \bar{r}_n)}{N^2(k_x)} F(k_x, z), \tag{37}$$

where

$$F(k_x, z) = \int_0^L dz'\ G(k_x, z, z')G^*(k_x, z_0, z'). \tag{38}$$

In the spatial domain,

$$E_{NR}(\bar{r}, \bar{r}_n) = \int_0^L dz' \int_{-\infty}^{\infty} dx'\ g(\bar{r}, \bar{r}')J_{NR}(\bar{r}', \bar{r}_n), \tag{39}$$

and

$$E_{MN}(\bar{r}, \bar{r}_n) = \int_{-\infty}^{\infty} dx'\ K(x - x', z)E_s(x', z_0, \bar{r}_n), \tag{40}$$

where

$$K(x, z) = \frac{1}{2\pi} \int_{-\infty}^{\infty} dk_x\ e^{ik_x x} \frac{1}{N^2(k_x)} F(k_x, z). \tag{41}$$

Note that

$$K(x, z_0) = \delta(x). \tag{42}$$

Inside the scatterer, the currents and fields are also related by the constitutive equation involving the unknown Q:

$$J_s(\bar{r}, \bar{r}_n; \omega) = Q(\bar{r}; \omega)E(\bar{r}, \bar{r}_n; \omega),$$

or

$$Q(\bar{r}; \omega) = J_s(\bar{r}, \bar{r}_n; \omega)/E(\bar{r}, \bar{r}_n; \omega), \tag{43}$$

where the dependence of all quantities on the frequency ω is now explicit. We will assume that Q has the following specific frequency dependence,

$$Q(\bar{r}; \omega) = \delta\sigma(\bar{r}) - i\omega\delta\varepsilon(\bar{r}), \tag{44}$$

where $\delta\sigma(\bar{r})$ and $\delta\varepsilon(\bar{r})$ do not depend on frequency. Below we will also assume that measurements are available at a finite number of frequencies, denoted by ω_m, $m = 1, \ldots, M$.

Equations (32), (35)–(37), (43), and (44) must all be consistent inside the scatterer. The minimum norm current J_{MN} and its associated field inside the scatterer E_{MN} are fixed by the data. Thus these equations can only be made consistent by adjusting Q and the nonradiating current J_{NR}. Specifically, (43) and (44) imply that, inside the scatterer, the electric field E_{NR} of the nonradiating currents, when added to E_b and E_{MN}, must give a total electric field that divides the scattering current J_s to produce a Q that does not depend on the position of the source $\bar{r}_n$ and depends on frequency only through the factor $i\omega$ (equation (44)). In the next sections we will show how to incorporate these conditions by expanding the nonradiating currents in suitable basis functions and minimizing two cost functions. First, we illustrate the above formulas for the model problem of Figure 1. In this model problem the weighting function $N^2(k_x)$ in (28) can be evaluated explicitly. For the measurement line $z_0 = 0$,

$$N^2(k_x) = \left(\frac{\omega\mu_0}{2|k_{bz}|}\right)^2 \frac{1 - e^{-2k''_{bz}L}}{2k''_{bz}}, \qquad k''_{bz} \neq 0, \tag{45a}$$

$$N^2(k_x) = \left(\frac{\omega\mu_0}{2k_{bz}}\right)^2 L, \qquad k''_{bz} = 0. \tag{45b}$$

The minimum norm solution can then be written explicitly in terms of the Fourier transform of the data,

$$\tilde{J}_{MN}(k_x, z', \bar{r}_n) = \frac{2k_{bz}}{\omega\mu_0} \frac{2k''_{bz}}{1 - e^{-2k''_{bz}L}} \cdot \tilde{E}_s(k_x, z_0, \bar{r}_n)e^{-ik^*_{bz}z'}, \qquad k''_{bz} \neq 0, \tag{46a}$$

$$\tilde{J}_{MN}(k_x, z', \bar{r}_n) = \frac{2k_{bz}}{\omega\mu_0} \frac{1}{L} \cdot \tilde{E}_s(k_x, z_0, \bar{r}_n)e^{-ik_{bz}z'}, \qquad k''_{bz} = 0. \tag{46b}$$

The electric field of the minimum norm currents can also be calculated explicitly in terms of the transformed data,

$$\tilde{E}_{MN}(k_x, z', \bar{r}_n) = \left[\frac{2k''_{bz}}{1 - e^{-2k''_{bz}L}} \frac{\sin(k'_{bz}z')}{k'_{bz}} e^{-k''_{bz}z} + \frac{1 - e^{-2k''_{bz}(L - z')}}{1 - e^{-2k''_{bz}L}} e^{-ik^*_{bz}z'}\right]\tilde{E}_s(k_x, z_0, \bar{r}_n), \qquad k''_{bz} \neq 0, \tag{47a}$$

$$\tilde{E}_{MN}(k_x, z', \bar{r}_n) = \left[\frac{1}{L} \frac{\sin(k_{bz}z')}{k_{bz}} + \left(1 - \frac{z'}{L}\right)e^{-ik_{bz}z'}\right] \cdot \tilde{E}_s(k_x, z_0, \bar{r}_n), \qquad k''_{bz} = 0. \tag{47b}$$

and

$$F(k_x, z) = \int_0^L dz'\ G(k_x, z, z')G^*(k_x, z_0, z'),$$

$$F(k_x, z) = \left(\frac{\omega\mu_0}{2|k_{bz}|}\right)^2 \left[\frac{\sin(k'_{bz}z)}{k'_{bz}} + \frac{1 - e^{-2k''_{bz}(L-z)}}{2k''_{bz}} e^{-ik'_{bz}z} e^{-k''_{bz}z}\right], \quad k''_{bz} \neq 0, \tag{48a}$$

$$F(k_x, z) = \left(\frac{\omega\mu_0}{2k_{bz}}\right)^2 \left[\frac{\sin(k_{bz}z)}{k_{bz}} + (L - z)e^{-ik_{bz}z}\right], \quad k''_{bz} = 0. \tag{48b}$$

5. Basis Functions for Nonradiating Currents

To solve for the nonradiating scattering currents, we must first expand these currents in suitable basis functions. This section describes basis functions that are strictly nonradiating (i.e., generate zero field everywhere outside their domain of support) and are thus suitable for continuous measurements. In reality, of course, the field can only be measured at a finite number of locations. Appendix A describes basis functions that produce zero field only at a finite number of points outside the scatterer and are thus suitable for discrete measurements. We call the basis functions for discrete measurements "invisible." While nonradiating basis functions are less general than invisible ones (every nonradiating source is an invisible source, but not vice versa), they have some convenient properties and are useful for studying the limit of continuous measurements.

Nonradiating sources can be explicitly constructed using a method first proposed by *Devaney and Wolf* [1973]. Let $\phi(\bar{r})$ be a function that vanishes outside some domain V but is otherwise arbitrary. Then the source distribution

$$\psi(\bar{r}; \omega) = -\frac{1}{i\omega\mu_0}[\nabla^2\phi(\bar{r}) + k_b^2\phi(\bar{r})], \tag{49}$$

is nonradiating; that is,

$$\int d\bar{r}'\, g(\bar{r}, \bar{r}'; \omega)\psi(\bar{r}'; \omega) = 0, \quad \bar{r} \notin V. \tag{50}$$

This property is easily proved by substituting (49) for ψ into (50), integrating by parts with Green's theorem, and using the fact that ϕ vanishes outside V. This proof also shows that the electric field of the nonradiating source ψ is just ϕ, the function that was operated on in (49). The normalization by $-i\omega\mu_0$ in (49) is for convenience: If ϕ has the units of electric field, then ψ will have the units of electric current. To yield a classical nonradiating source, the function ϕ must have continuous first and second partial derivatives up to the boundary of the domain V. Then, by construction the electric field of the source ψ in (49) is zero and has zero normal derivative on the boundary of the domain V:

$$\phi(\bar{r}) = 0, \quad \text{and} \quad \frac{\partial\phi}{\partial n}(\bar{r}) = 0, \quad \bar{r} \in \partial V. \tag{51}$$

The restrictions on the continuity of ϕ can be relaxed, however, if (49)–(51) are all interpreted in a weak or distributional sense.

Now let $\phi_l(\bar{r})$, $l = 1, \ldots, L$, be a linearly independent set of functions that vanish outside the scatterer and generate a new set of functions $\psi_l(\bar{r}; \omega)$ by

$$\psi_l(\bar{r}; \omega) = -\frac{1}{i\omega\mu_0}[\nabla^2\phi_l(\bar{r}) + k_b^2\phi_l(\bar{r})], \quad l = 1, \ldots, L. \tag{52}$$

If the functions ϕ_l are chosen properly, then the functions ψ_l will also be linearly independent and suitable for the expansion of a general nonradiating current,

$$J_{NR}(\bar{r}, \bar{r}_n; \omega_m) = \sum_l a_l^{(nm)}\psi_l(\bar{r}; \omega_m), \tag{53}$$

where $a_l^{(nm)}$ are coefficients to be determined in solving the inverse scattering problem. The electric field generated by this J_{NR} is just

$$E_{NR}(\bar{r}, \bar{r}_n; \omega_m) = \sum_l a_l^{(nm)}\phi_l(\bar{r}). \tag{54}$$

Thus with the basis functions given by (52), no further computation is needed to obtain the electric field.

It is easy to construct sets of functions ϕ_l with the properties required above. Except, however, for simple domains such as the sphere [*Gamliel et al.*, 1989], it is hard to construct a set of functions ψ_l that are complete and can represent an arbitrary nonradiating current. Here we give an example of local nonradiating basis functions based on piecewise "cubic Bessel" interpolation (a variant of cubic Hermite interpolation; see *Conte and de Boor* [1980]) on a gridded rectangular domain. These

basis functions are complete in the finite element sense; that is, they can represent any nonradiating source and its field in the limit as the grid spacing $h \to 0$. This construction for rectangular domains can be extended to general domains with Hermite finite elements.

Let the domain of the scatterer be covered with a uniform rectangular grid,

$$\bar{r}_{pq} = (x_p, z_q), \quad x_p = x_0 + ph, \quad z_q = z_0 + qh,$$

where $p = 0, \ldots, P+1$, and $q = 0, \ldots, Q+1$. A basis function $\phi_{pq}(\bar{r})$ is assigned to each interior node, $p = 1, \ldots, P$, and $q = 1, \ldots, Q$, as the product,

$$\phi_{pq}(\bar{r}) = \varphi(x - x_p)\varphi(z - z_q), \tag{55}$$

where φ is the piecewise cubic polynomial,

$$\varphi(\xi) = \varphi_0(\xi) + \frac{1}{2h}[\varphi_1(\xi + h) - \varphi_1(\xi - h)], \tag{56}$$

with

$$\varphi_0(\xi) = (|\xi/h| - 1)^2(2|\xi/h| + 1), \quad -h < \xi < h,$$
$$\varphi_0(\xi) = 0 \qquad \text{otherwise},$$

and

$$\varphi_1(\xi) = \xi(|\xi/h| - 1)^2, \quad -h < \xi < h,$$
$$\varphi_1(\xi) = 0 \qquad \text{otherwise}.$$

The piecewise cubic polynomial $\varphi(\xi)$ is continuous with continuous first derivative; its support is the interval $-2h < \xi < 2h$; $\varphi(0) = 1$, $\varphi(-h) = \varphi(h) = 0$; and its derivative $\varphi'(0) = 0$, while $\varphi'(-h) = 1$ and $\varphi'(h) = -1$. Thus the function

$$f(\xi) = \sum_l f_l \varphi(\xi - \xi_l), \qquad \xi_l = lh,$$

is continuous with continuous first derivative; its value at a node ξ_l is the sample value, $f(\xi_l) = f_l$; and its derivative at a node is the central difference approximation, $f'(\xi_l) = (f_{l+1} - f_{l-1})/(2h)$.

The functions ϕ_{pq} are tensor products of piecewise polynomials in x and z and have properties in two dimensions similar to those listed above. After renumbering the nodes with a single index (e.g., $l = (p-1)Q + q$) the resulting functions $\phi_{pq} \to \phi_l$ then generate nonradiating basis functions through (52) and the expansion for J_{NR} via (53). The coefficients $a_l^{(nm)}$ are now just the values of E_{NR} at the nodes $\bar{r}_{pq}$. The nonradiating basis functions generated by the ϕ_{pq} will be discontinuous (because the ϕ_{pq} have only continuous first derivatives). Nevertheless, the boundary condition of (51) can still be satisfied in the strong sense by only assigning basis functions to interior nodes of the grid and by dropping the first term in brackets in (56) for nodes along the lines $x = x_1$ and $z = z_1$ and the second term for nodes along the lines $x = x_Q$ and $z = z_P$.

6. An Inversion Algorithm

To implement the inversion for the nonradiating scattering currents and, ultimately, the inversion for Q, we define two cost functions. The first cost function enforces consistency of Q, J, and E at any given point inside the scatterer as the source position and frequency varies. It expresses the condition that the material property Q is independent of source position and has a simple prescribed frequency dependence:

$$C_1(Q', Q'') = \sum_{n,m} |J_s(\bar{r}, \bar{r}_n; \omega_m) - Q(\bar{r}; \omega_m)E(\bar{r}, \bar{r}_n; \omega_m)|^2$$

$$= \sum_{n,m} |J_s(\bar{r}, \bar{r}_n; \omega_m) - [Q'(\bar{r}) + i\omega_m Q''(\bar{r})]E(\bar{r}, \bar{r}_n; \omega_m)|^2, \tag{57}$$

where

$$Q'(\bar{r}) = \delta\sigma(\bar{r}),$$

$$Q''(\bar{r}) = -\delta\varepsilon(\bar{r}).$$

As before, E and J are split into their different parts:

$$E(\bar{r}, \bar{r}_n; \omega_m) = E_b(\bar{r}, \bar{r}_n; \omega_m) + E_{MN}(\bar{r}, \bar{r}_n; \omega_m) + E_{NR}(\bar{r}, \bar{r}_n; \omega_m),$$

$$J_s(\bar{r}, \bar{r}_n; \omega_m) = J_{MN}(\bar{r}, \bar{r}_n; \omega_m) + J_{NR}(\bar{r}, \bar{r}_n; \omega_m).$$

The second cost function enforces consistency in the spatial variation of J, E, and Q inside the scatterer for a given source position and frequency:

$$C_2(a_l^{(nm)}) = \int d\bar{r}\, |J_s(\bar{r}, \bar{r}_n; \omega_m) - Q(\bar{r}; \omega_m)E(\bar{r}, \bar{r}_n; \omega_m)|^2$$

$$= \int d\bar{r} \left| J_{MN}(\bar{r}, \bar{r}_n; \omega_m) + \sum_l a_l^{(nm)} \psi_l(\bar{r}; \omega_m) \right.$$

$$- Q(\bar{r}; \omega_m)[E_b(\bar{r}, \bar{r}_n; \omega_m) + E_{MN}(\bar{r}, \bar{r}_n; \omega_m)$$

$$\left. + \sum_l a_l^{(nm)} \phi_l(\bar{r}; \omega_m)] \right|^2. \quad (58)$$

The integration above is over the domain of the scatterer (or the unknown region). The second equality comes from decomposing J and E into their different parts and using the expansions (53) and (54) for the nonradiating current J_{NR} and its associated field E_{NR}. Minimization of the first cost function by varying Q gives

$$Q(\bar{r}; \omega) = \frac{\sum_{n,m} \text{Re}\,\{J_s(\bar{r}, \bar{r}_n; \omega_m) E^*(\bar{r}, \bar{r}_n; \omega_m)\}}{\sum_{n,m} |E(\bar{r}, \bar{r}_n; \omega_m)|^2}$$

$$+ i\omega \frac{\sum_{n,m} \omega_m \text{Im}\,\{J_s(\bar{r}, \bar{r}_n; \omega_m) E^*(\bar{r}, \bar{r}_n; \omega_m)\}}{\sum_{n,m} \omega_m^2 |E(\bar{r}, \bar{r}_n; \omega_m)|^2}. \quad (59)$$

This formula for $Q(\bar{r}; \omega)$ uses all the data: all source positions, receiver positions (in the computation of the backpropagated fields), and frequencies. The current J_s and electric field E on the right-hand side include the nonradiating part of the current distribution and its associated electric field inside the scatterer, which depend on the expansion coefficients $a_l^{(nm)}$ that have not yet been fixed.

These coefficients are chosen to minimize the second cost function. Minimization of C_2 by varying $a_l^{(nm)}$ gives the following matrix equation for each source position $\bar{r}_n$ and frequency ω_m,

$$\sum_q B_{lq}(\omega_m) a_q^{(nm)} = -c_l(\bar{r}_n; \omega_m),$$

or

$$\bar{\bar{B}}(\omega_m) \cdot \bar{a}_{nm} = -\bar{c}(\bar{r}_n; \omega_m). \quad (60)$$

Here $\bar{\bar{B}}(\omega_m)$ is a Hermitian matrix with elements

$$B_{lq}(\omega_m) = \int d\bar{r}\, [\psi_l^*(\bar{r}; \omega_m) - Q^*(\bar{r}; \omega_m)\phi_l^*(\bar{r}; \omega_m)]$$

$$\cdot [\psi_q(\bar{r}; \omega_m) - Q(\bar{r}; \omega_m)\phi_q(\bar{r}; \omega_m)], \quad (61)$$

$\bar{a}_{nm}$ is a vector of the expansion coefficients $a_l^{(nm)}$, and $\bar{c}(\bar{r}_n; \omega_m)$ is the vector with elements

$$c_l(\bar{r}_n; \omega_m) = \int d\bar{r}\, \{J_{MN}(\bar{r}, \bar{r}_n; \omega_m)$$

$$- Q(\bar{r}; \omega_m)[E_b(\bar{r}, \bar{r}_n; \omega_m) + E_{MN}(\bar{r}, \bar{r}_n; \omega_m)]\}$$

$$\cdot [\psi_l^*(\bar{r}; \omega_m) - Q^*(\bar{r}; \omega_m)\phi_l^*(\bar{r}; \omega_m)]. \quad (62)$$

The matrix $\bar{\bar{B}}(\omega_m)$ depends only on the frequencies of operation ω_m; thus different source positions at the same frequency do not require much extra computation. Also, if localized basis functions are used, $\bar{\bar{B}}(\omega_m)$ is sparse. Ideally, the two cost functions would be minimized simultaneously by varying both Q and $a_l^{(nm)}$, but this simultaneous minimization is a nonlinear problem. The minimization by varying Q and $a_l^{(nm)}$ sequentially suggests the following iterative scheme for the full nonlinear minimization:

1. Approximate $J_s(\bar{r}, \bar{r}_n; \omega_m)$ and $E(\bar{r}, \bar{r}_n; \omega_m)$ by

$$J_s(\bar{r}, \bar{r}_n; \omega_m) = J_{MN}(\bar{r}, \bar{r}_n; \omega_m),$$

$$E(\bar{r}, \bar{r}_n; \omega_m) = E_b(\bar{r}, \bar{r}_n; \omega_m) + E_{MN}(\bar{r}, \bar{r}_n; \omega_m).$$

2. Invert for $Q(\bar{r}; \omega_m)$ from (59) employing all data available.
3. Construct the matrix $\bar{\bar{B}}(\omega_m)$ and the vector $\bar{c}(\bar{r}_n; \omega_m)$ from (61)–(62).
4. Invert for the coefficients $a_l^{(nm)}$ from (60).
5. Compute the total induced current $J_s(\bar{r}, \bar{r}_n; \omega_m)$ and the internal electric field $E(\bar{r}, \bar{r}_n; \omega_m)$ and return to step (2). The iteration is continued until changes in the profile are less than some specified tolerance.

The above algorithm is, in effect, an alternating direction minimization scheme for the full cost function,

$$C(Q, a_l^{(nm)}) = \int d\bar{r} \sum_{n,m} |J_s(\bar{r}, \bar{r}_n; \omega_m)$$

$$- Q(\bar{r}; \omega_m)E(\bar{r}, \bar{r}_n; \omega_m)|^2, \quad (63)$$

$$C(Q, a_l^{(nm)}) = \sum_{n,m} \int d\bar{r}\, |J_s(\bar{r}, \bar{r}_n; \omega_m)$$

$$- Q(\bar{r}; \omega_m)E(\bar{r}, \bar{r}_n; \omega_m)|^2. \quad (64)$$

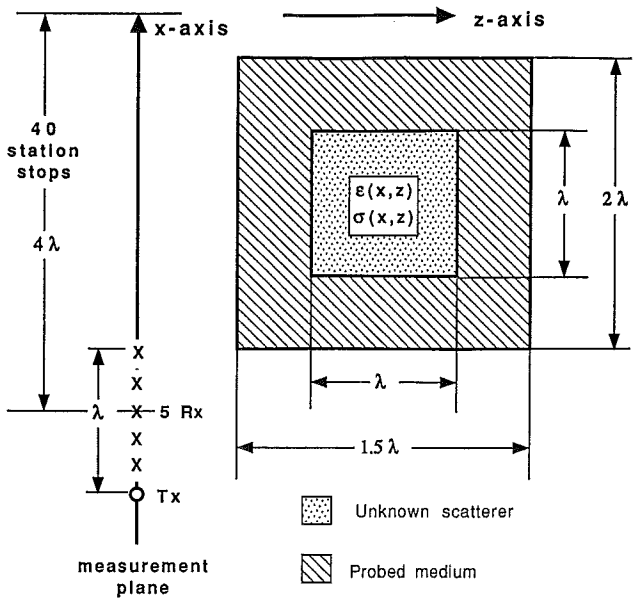

Figure 2. Geometry and model for the first example.

Minimization of the first cost function $C_1(Q', Q'')$ by varying Q is a pointwise minimization of the integrand (in (63)) of this full cost function, whereas minimization of the second cost function $C_2(a_l^{(nm)})$ by varying $a_l^{(nm)}$ is a pointwise minimization of the summand (in (64) when the order of integration and summation are interchanged). This scheme is stable because the value of the cost function $C(Q, a_l^{(nm)})$ is never increased by either minimization step. Finally, Appendix C shows how to modify the cost function C_1 so that the reconstructed conductivity and electric susceptibility are positive functions.

7. Results

Figure 2 shows the first model problem on which we tested the inversion algorithm described above. The scatterer (the dotted region) is a 2-D square cylinder of dimensions $\lambda \times \lambda$, where λ is the wavelength of the background medium (experiments were simulated at a single frequency). The background has a relative permittivity of 10 and a loss tangent (defined as $\sigma/\omega\varepsilon_0$) of 10. The relative permittivity of the scatterer is 50, and the loss tangent is 50 (a contrast in material properties of 1:5). Synthetic data for an electric line source

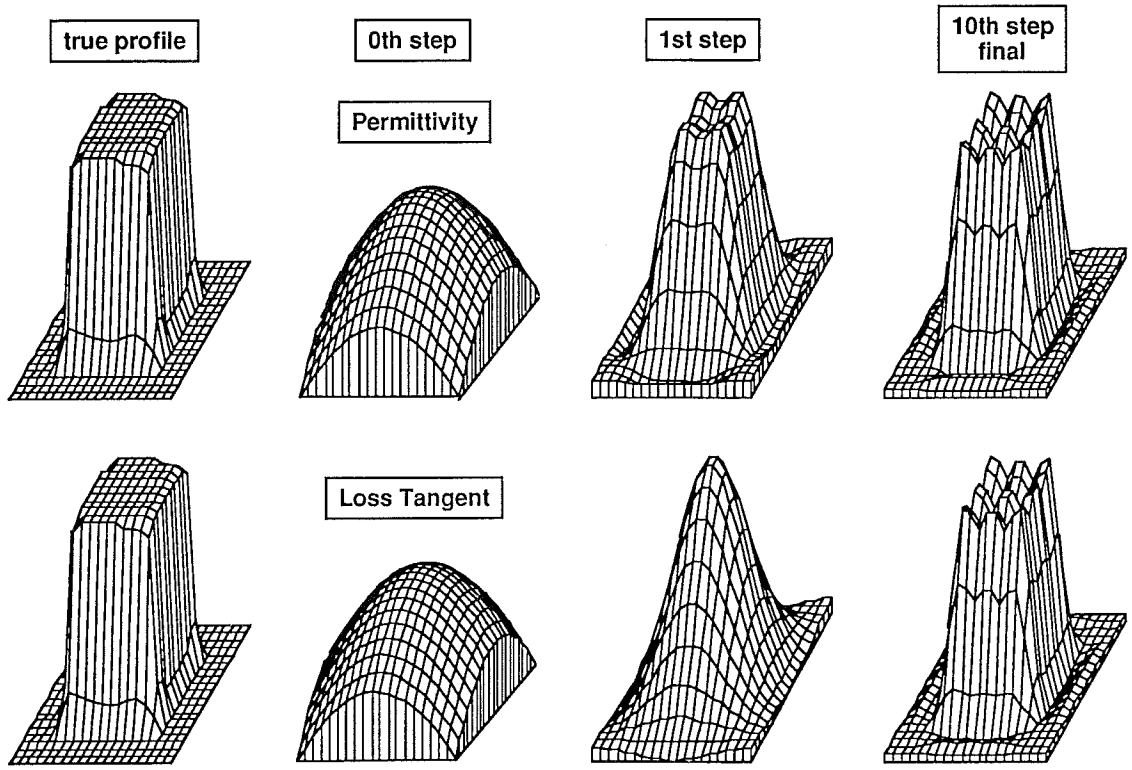

Figure 3. Reconstructed permittivity and conductivity maps. Contrast = 1:5, number of grid points = 7 × 7.

excitation of the medium were generated by the method of moments. The data are the y component of the electric field at five positions equally spaced out to a distance λ from the transmitter. The transmitter-receiver array is moved over a distance 4λ, centered about the scatterer, in 40 steps.

The hatched region in Figure 2 is the unknown region where the material properties were allowed to vary in the inversion. This region is divided into a grid of 7×7 points. The unknowns are the permittivity and conductivity (expressed as the loss tangent). The inversion uses invisible basis functions constructed from sinc functions [*Tracy and Johnson,* 1983; *Johnson et al.*, 1984; *Cavicchi et al.*, 1988] according to the algorithm described in section 2 of Appendix A. Except for numerical error, the data were noise-free.

Figure 3 shows the reconstruction after the zeroth, first, and last (tenth) iteration of the algorithm. The smooth reconstruction at the zeroth step comes from the minimum norm inversion for the scattering currents. The reconstruction after the first step already reasonably defines the scatterer. Further iterations sharpen the picture somewhat; the final result is a spatially filtered version of the actual model. This filtering is characteristic of any inverse scattering problem that operates at a single frequency.

Figure 4 shows a second model problem which consists of a 2-D square cylinder of dimensions $1.5\lambda \times 1.5\lambda$. Both the permittivity and conductivity vary smoothly inside the scatterer starting from the background values at the edges of the cylinder and varying sinusoidally in the interior. The background medium is lossless and has a relative permittivity of 5. The maximum relative permittivity of the scatterer is 50 (a maximum contrast of 1:10) and a maximum loss tangent of 50. As in the first example, the data are generated synthetically for an electric line source and are noise-free. The data are the y component of the electric field at five positions equally spaced out to a distance λ from the transmitter. The transmitter-receiver array is moved over a distance 2.5λ, centered about the scatterer, in 20 steps. In this example we assume that the boundaries of the scatterer are known, and the objective is to reconstruct the permittivity and conductivity variations inside the scatterer. The scatterer is divided into a grid of 5×5 points. The nonradiating currents are expanded using the invisible basis functions constructed from sinc functions

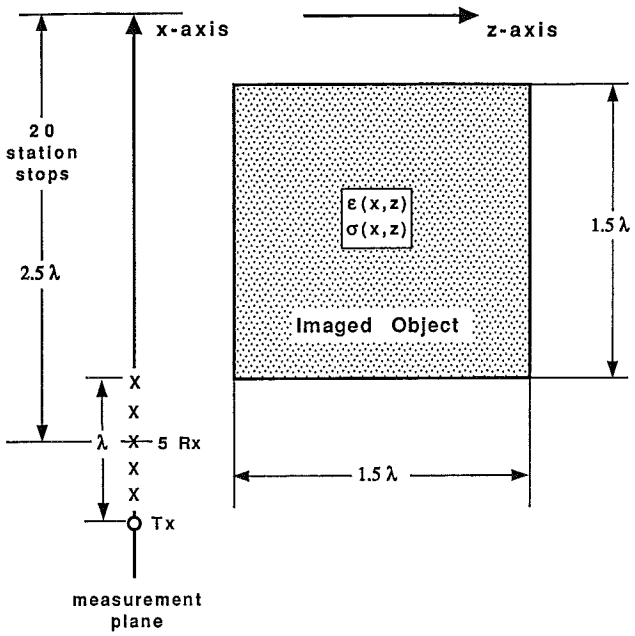

Figure 4. Schematic of the inversion problem for the second example.

according to the algorithm described in section 1 of Appendix A. Figure 5 shows the reconstructions at the first three iterations and the last (sixth) where the rms error in the inverted permittivity and conductivity is less than 1%.

8. Conclusions

The STIE method described here casts the nonlinear inverse scattering problem as the solution of a coupled set of linear equations. The method is iterative but does not proceed by matching the data better at successive steps. Instead, the data is matched at the initial step through the solution of an inverse source problem for the minimum norm or radiating part of the scattering currents. The iterative part of the algorithm then seeks an electric field and material properties inside the scatterer that are consistent with the incident electric field and the field of the minimum norm scattering currents. The iterations proceed by sequentially adjusting the material properties and the nonradiating scattering currents. A key part of the algorithm is the use of explicit nonradiating (or invisible) basis functions.

Several issues still need to be addressed with the STIE method. First is the sensitivity of the method to noise in the data and to the number of unknowns that are used in the solutions for both the minimum

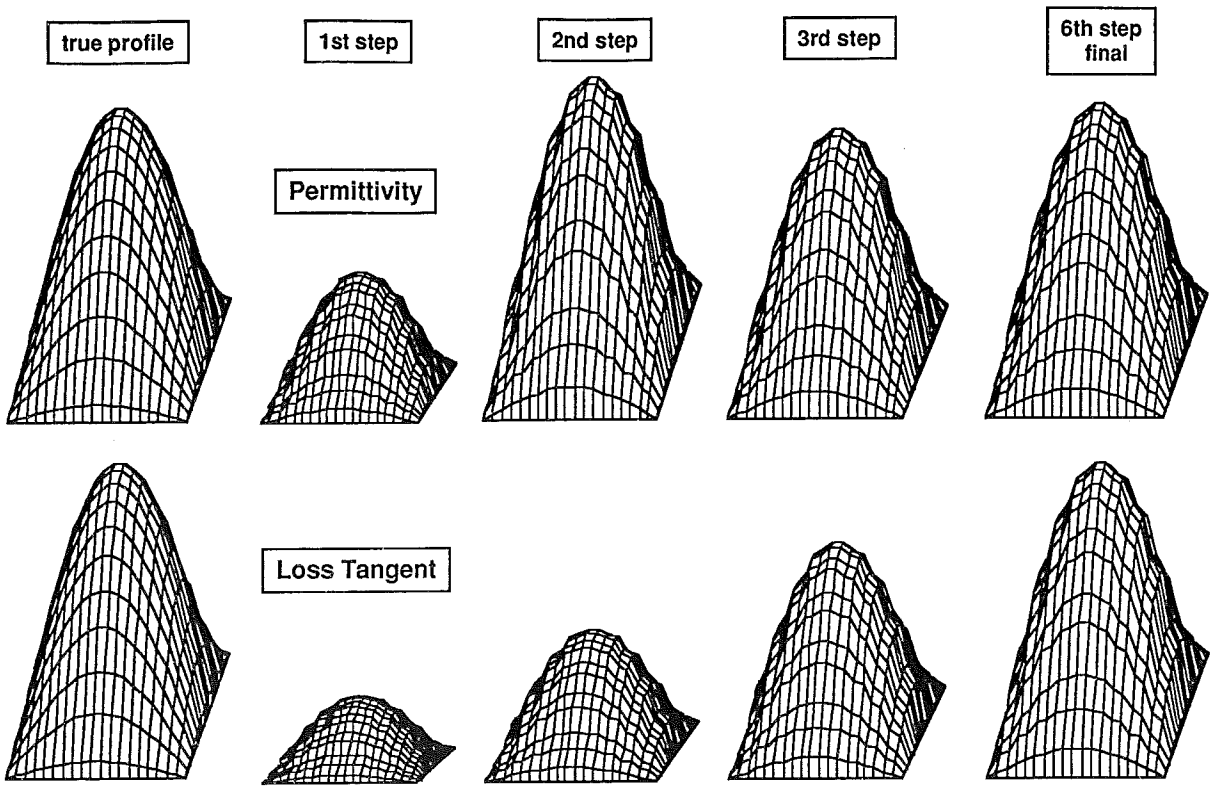

Figure 5. Reconstructed permittivity and conductivity maps. Contrast = 1:10, number of grid points = 5 × 5.

norm and nonradiating currents. Next is the sufficiency of the constraints that are imposed on the nonradiating sources to provide a unique reconstruction. Finally, there is need for an estimate of the rate of convergence of this method.

Appendix A: Discrete Measurements

The methods described in the text apply to idealized continuous measurements and require two modifications for discrete measurements: first, in the construction of the minimum norm currents, and second, in the construction of the nonradiating basis functions. The first modification is a standard application of Backus-Gilbert theory [*Aki and Richards*, 1980]. The second modification involves the notion of invisible sources, which are sources that generate zero field only at a finite set of points outside the scatterer. The first part of this appendix describes these modifications. The second part describes an alternative fully discrete method that deals directly with the electric field, instead of the currents, inside the scatterer.

A1. Expansions of the Currents

Assume that measurements are only available at a finite set of points, $\bar{r}_k = x_k\hat{x} + z_0\hat{z}$, $k = 1, \ldots, K$. Clearly, the operations described in section 3 (involving Fourier transforms, etc.) cannot be done directly on these data. To construct a discrete version, we start with the equations,

$$E_s(\bar{r}_k, \bar{r}_n) = \int_V d\bar{r}'\, g(\bar{r}_k, \bar{r}')J_s(\bar{r}', \bar{r}_n), \qquad k = 1, \ldots, K. \tag{65}$$

A minimum norm solution of these equations can be obtained by expanding J_s in the discrete set of basis functions given by the conjugate of the kernels $g(\bar{r}_k, \bar{r}')$:

$$J_{MN}(\bar{r}', \bar{r}_n) = \sum_j c_j g^*(\bar{r}_j, \bar{r}'). \tag{66}$$

Substituting into (65) gives a matrix equation for the coefficients c_j,

$$\sum_{j=1}^{K} \mathcal{G}_{kj} c_j = E_s(\bar{r}_k, \bar{r}_n), \tag{67}$$

where

$$\mathcal{G}_{kj} = \int_V d\bar{r}'\, g(\bar{r}_k, \bar{r}') g^*(\bar{r}_j, \bar{r}'). \tag{68}$$

Thus if the matrix $\mathcal{G}$ is invertible,

$$c_j = \sum_k \mathcal{G}^{-1}_{jk} E_s(\bar{r}_k, \bar{r}_n), \tag{69}$$

and (66) gives the minimum norm currents. If $\mathcal{G}$ is not invertible, its generalized inverse can be used. The correspondence between this discrete version and the continuous version in the text is straightforward.

We now construct current basis functions that will give zero field at the measurement locations, $\bar{r}_k$, $k = 1, \ldots, K$. We first choose a set of M radiating basis functions with $M > K$. Let $L = M - K$, and split these basis functions into two sets:

$$\bar{\psi}^{(1)}_j(\bar{r}), j = 1, \ldots, K; \quad \bar{\psi}^{(2)}_l(\bar{r}), \qquad l = 1, \ldots, L.$$

Let $\bar{\phi}$ be the electric field generated by each basis function,

$$\bar{\phi}^{(1,2)}_{(j,l)}(\bar{r}; \omega) = \int d\bar{r}'\, g(\bar{r}, \bar{r}') \bar{\psi}^{(1,2)}_{(j,l)}(\bar{r}'),$$

where the dependence of $\bar{\phi}$ on frequency ω comes from the Green function. Next, form the $K \times K$ and $K \times L$ matrices $\Phi^{(1)}(\omega)$ and $\Phi^{(2)}(\omega)$, whose elements are

$$\Phi^{(1)}_{kj}(\omega) = \bar{\phi}^{(1)}_j(\bar{r}_k; \omega) = \int d\bar{r}'\, g(\bar{r}_k, \bar{r}') \bar{\psi}^{(1)}_j(\bar{r}'), \tag{70}$$

$$k = 1, \ldots, K, \quad j = 1, \ldots, K,$$

$$\Phi^{(2)}_{kl}(\omega) = \bar{\phi}^{(2)}_l(\bar{r}_k; \omega) = \int d\bar{r}'\, g(\bar{r}_k, \bar{r}') \bar{\psi}^{(2)}_l(\bar{r}'), \tag{71}$$

$$k = 1, \ldots, K, \quad l = 1, \ldots, L.$$

The kjth element of the matrix $\Phi^{(1)}$ is just the electric field at the kth receiver location that is generated by the jth basis function in the first set of basis functions. A similar interpretation holds for the elements $\Phi^{(2)}_{kl}$.

If the basis functions are chosen properly (radiating), the $K \times K$ matrix $\Phi^{(1)}(\omega)$ will have an inverse, which we denote by $\Phi^{-(1)}(\omega)$. Define new basis functions, ψ_l, $l = 1, \ldots, L$, as the following linear combination of the original basis functions:

$$\psi_l(\bar{r}; \omega) = \bar{\psi}^{(2)}_l(\bar{r}) - \sum_j \sum_k \bar{\psi}^{(1)}_j(\bar{r}) \Phi^{-(1)}_{jk}(\omega) \Phi^{(2)}_{kl}(\omega), \tag{72}$$

$$l = 1, \ldots, L.$$

It is easy to show that these new basis functions give zero electric field at the receiver locations $\bar{r}_k$.

The $L = M - N$ invisible basis functions constructed in this way can replace the nonradiating basis functions in the expansion,

$$J_{NR}(\bar{r}, \bar{r}_n; \omega_m) = \sum_l a^{(nm)}_l \psi_l(\bar{r}; \omega_m). \tag{73}$$

As in the text, the unknown coefficients $a^{(nm)}_l$ are determined by minimizing the cost function C_2. Each of the new basis functions generates an (nonzero) electric field ϕ_l inside the scatterer,

$$\phi_l(\bar{r}; \omega_m) = \int d\bar{r}'\, g(\bar{r}, \bar{r}') \psi_l(\bar{r}'; \omega_m); \tag{74}$$

thus

$$E_{NR}(\bar{r}, \bar{r}_n; \omega_m) = \sum_l a^{(nm)}_l \phi_l(\bar{r}; \omega_m). \tag{75}$$

A2. Expansions of the Internal Electric Field

We now describe a fully discrete version of the STIE method that uses expansions of the electric field, instead of the current, inside the scatterer. This approach is useful for dealing with discontinuous material properties, because a finite set of smooth basis functions will represent the electric field, which is continuous in the TE polarization, more accurately than the current, which is discontinuous. The expansion can still preserve the distinction between the radiating and nonradiating parts of the field.

Let the total electric field inside the scatterer be given by

$$E(\bar{r}, \bar{r}_n; \omega_m) = \sum_i c^{(nm)}_i \bar{\psi}_i(\bar{r}), \tag{76}$$

where the $\bar{\psi}_i$ are the basis functions and $c^{(nm)}_i$ are the expansion coefficients. As before, the superscript (nm) indicates dependence on source position

$\bar{r}_n$ and frequency ω_m. The scattering current generated by this electric field is

$$J_s(\bar{r}, \bar{r}_n; \omega_m) = Q(\bar{r}; \omega_m) \sum_i c_i^{(nm)} \bar{\psi}_i(\bar{r}); \quad (77)$$

in turn, the scattered field generated by this current is

$$E_s(\bar{r}, \bar{r}_n; \omega_m) = \sum_i c_i^{(nm)} \bar{\phi}_i(\bar{r}; \omega_m). \quad (78)$$

where

$$\bar{\phi}_i(\bar{r}; \omega_m) = \int d\bar{r}'\, g(\bar{r}, \bar{r}') Q(\bar{r}'; \omega_m) \bar{\psi}_i(\bar{r}'). \quad (79)$$

In a forward problem, enforcing consistency of the two expansions, (76) and (77) (plus the incident field E_b), inside the scatterer leads to the standard method-of-moments solution for the coefficients $c_i^{(nm)}$. In the inverse problem, however, we require the expansion to be consistent with the measured electric field outside the scatterer (the data), and we also wish to maintain the distinction between the radiating and nonradiating parts of the internal field. As in the previous section, we thus select M basis functions, where $M > K$ (K is the number of receiver locations at a given source location and frequency), and we split these basis functions into two sets such that

$$E(\bar{r}, \bar{r}_n; \omega_m) = \sum_{j=1}^{K} \bar{\psi}_j^{(1)}(\bar{r}) b_j^{(nm)} + \sum_{l=1}^{L} \bar{\psi}_l^{(2)}(\bar{r}) a_l^{(nm)}, \quad (80)$$

where $L = M - N$. The functions $\bar{\phi}_i$ also naturally split into two sets according to (79). The goal now is to eliminate the first set of coefficients $b_j^{(nm)}$ in (80) by matching the data; this will leave the second set of coefficients $a_l^{(nm)}$ free to represent the nonradiating part of the field inside the scatterer.

Define the matrices,

$$\Phi_{kj}^{(1)}(\omega) = \bar{\phi}_j^{(1)}(\bar{r}_k; \omega), \quad k = 1, \ldots, K, \quad j = 1, \ldots, K, \quad (81)$$

$$\Phi_{kl}^{(2)}(\omega) = \bar{\phi}_l^{(2)}(\bar{r}_k; \omega), \quad k = 1, \ldots, K, \quad l = 1, \ldots, L, \quad (82)$$

whose elements are the scattered electric fields at the measurement locations generated by the basis functions in each set. We can then write for the scattered electric field at the measurement locations,

$$\sum_j \Phi_{kj}^{(1)}(\omega) b_j^{(nm)} + \sum_l \Phi_{kl}^{(2)}(\omega) a_l^{(nm)} = E_s(\bar{r}_k, \bar{r}_n; \omega_m). \quad (83)$$

If the basis functions are chosen properly, the matrix $\Phi^{(1)}(\omega)$ will have an inverse, so that $b_j^{(nm)}$ can be eliminated from this equation,

$$b_j^{(nm)} = \sum_k \Phi_{jk}^{-(1)}(\omega) \left[E_s(\bar{r}_k, \bar{r}_n; \omega_m) - \sum_l \Phi_{kl}^{(2)}(\omega) a_l^{(nm)} \right]. \quad (84)$$

Substituting back into the original expansion for E gives

$$E(\bar{r}, \bar{r}_n; \omega_m) = \sum_j \sum_k \bar{\psi}_j^{(1)}(\bar{r}) \Phi_{jk}^{-(1)}(\omega) E_s(\bar{r}_k, \bar{r}_n; \omega_m) + \sum_l \left[\bar{\psi}_l^{(2)}(\bar{r}) - \sum_j \sum_k \bar{\psi}_j^{(1)}(\bar{r}) \Phi_{jk}^{-(1)}(\omega) \Phi_{kl}^{(2)}(\omega) \right] a_l^{(nm)}. \quad (85)$$

The first term on the right-hand side of (85) is an electric field inside the scatterer that, when multiplied by Q and propagated by the Green function, exactly reproduces the measurements. The first term thus corresponds to E_{MN}, the minimum norm or radiating part of the electric field (with respect to the chosen basis functions),

$$E_{MN}(\bar{r}, \bar{r}_n; \omega_m) \equiv \sum_j \sum_k \bar{\psi}_j^{(1)}(\bar{r}) \Phi_{jk}^{-(1)}(\omega) E_s(\bar{r}_k, \bar{r}_n; \omega_m). \quad (86)$$

The second term on the right-hand side of (85) is an electric field inside the scatterer that radiates zero field at the measurement locations. The quantity in brackets in this term defines new basis functions for the invisible part of the field,

$$\psi_l(\bar{r}; \omega_m) \equiv \bar{\psi}_l^{(2)}(\bar{r}) - \sum_j \sum_k \bar{\psi}_j^{(1)}(\bar{r}) \Phi_{jk}^{-(1)}(\omega) \Phi_{kl}^{(2)}(\omega). \quad (87)$$

These basis functions are similar to the invisible basis functions described in the previous section, but their definition (and computation) involves the material property Q through (79). Finally, to obtain an iterative process for choosing the free coefficients $a_l^{(nm)}$, let ϕ_l and $\bar{E}_{MN}$ be the electric field generated by ψ_l and E_{MN} inside the scatterer by the action of the Green function; that is,

$$\phi_l(\bar{r};\omega_m) \equiv \int d\bar{r}'\, g(\bar{r},\bar{r}')Q(\bar{r}';\omega_m)\psi_l(\bar{r}';\omega_m), \tag{88}$$

and

$$\bar{E}_{MN}(\bar{r},\bar{r}_n;\omega_m) \equiv \int d\bar{r}'\, g(\bar{r},\bar{r}')Q(\bar{r}';\omega_m)E_{MN}(\bar{r}',\bar{r}_n;\omega_m). \tag{89}$$

The cost function of (58) now becomes

$$\begin{aligned} C_2(a_l^{(nm)}) &= \int d\bar{r}\, |J_s(\bar{r},\bar{r}_n;\omega_m) \\ &\quad - Q(\bar{r};\omega_m)E(\bar{r},\bar{r}_n;\omega_m)|^2 \\ &= \int d\bar{r}\, |Q(\bar{r};\omega_m)|^2 \Bigg| E_{MN}(\bar{r},\bar{r}_n;\omega_m) \\ &\quad + \sum_l a_l^{(nm)}\psi_l(\bar{r};\omega_m) \\ &\quad - \Bigg[E_b(\bar{r},\bar{r}_n;\omega_m) + \bar{E}_{MN}(\bar{r},\bar{r}_n;\omega_m) \\ &\quad + \sum_l a_l^{(nm)}\phi_l(\bar{r};\omega_m)\Bigg]\Bigg|^2. \end{aligned} \tag{90}$$

Minimization of this cost function leads to a matrix equation for the coefficients $a_l^{(nm)}$, similar to (59). The cost function C_1 remains the same. Thus the iterative minimization outlined in the text can proceed by expansions of the electric field instead of the scattering current. A disadvantage of this approach is that the functions ψ_l and ϕ_l now depend on the material properties Q and must be updated during the iterations.

Appendix B: Minimum-Norm Scattering Currents and the Resolution Kernel

The minimum norm solution for the scattering currents, derived in section 3, is

$$\tilde{J}_{MN}(k_x, z', \bar{r}_n) = \frac{\tilde{E}_s(k_x, z_0, \bar{r}_n)}{N^2(k_x)} G^*(k_x, z_0, z').$$

The scattering currents given by the minimum norm solution always lie in the space spanned by $G^*(k_x, z_0, z')$; the projections along this basis are determined by the scattered field $\tilde{E}_s(k_x, z_0, \bar{r}_n)$ at different transmitter locations $\bar{r}_n$.

To derive the relationship between the minimum norm solution and the actual induced currents, substitute (19) into (27) and express both $\tilde{J}_{MN}(k_x, z', \bar{r}_n)$ and $\tilde{J}_s(k_x, z', \bar{r}_n)$ in the spatial domain:

$$\begin{aligned} J_{MN}(\bar{r},\bar{r}_n) &= \int_0^L dz' \int_{-\infty}^{\infty} dx' \\ &\quad \cdot \mathcal{R}(x-x', z, z')J_s(x', z', \bar{r}_n). \end{aligned} \tag{91}$$

Here $\mathcal{R}(x - x', z, z')$ is the resolution kernel of the inversion operator that gives the minimum norm current in terms of the actual scattering current (the resolution kernel is also called the point spread function) and is given by

$$\begin{aligned} \mathcal{R}(x'-x'', z', z'') &= \frac{1}{2\pi}\int_{-\infty}^{\infty} dk_x\, e^{ik_x(x'-x'')} \frac{1}{N^2(k_x)} \\ &\quad \cdot G^*(k_x, z_0, z')G(k_x, z_0, z''), \\ &= \frac{2}{\pi}\int_0^{\infty} dk_x \cos\{k_x(x'-x'')\} \\ &\quad \cdot \frac{k''_{bz}}{1-e^{-2k''_{bz}L}} e^{-k''_{bz}(z'+z'')} e^{-ik_{bz}(z'-z'')}. \end{aligned} \tag{92}$$

The resolution kernel $\mathcal{R}(x - x', z, z')$ has the following properties:

1. Its support, in general, is the entire $x - z$ space and not just the domain of the scatterer.
2. It is a convolutional operator in the direction parallel to the measurement plane; that is, along the x axis.
3. It is symmetric in the plane parallel to the measurement plane:

$$\mathcal{R}(x-x', z, z') = \mathcal{R}(x'-x, z, z').$$

4. It is a self-adjoint operator:

$$\mathcal{R}(x-x', z, z') = \mathcal{R}^*(x'-x, z', z).$$

5. The function $g(x, z_0, \bar{r}')$ is an eigenfunction of $\mathcal{R}(x' - x'', z', z'')$ with a unity eigenvalue:

$$\int_0^L dz' \int_{-\infty}^{\infty} dx'\, \mathcal{R}(x'-x'', z', z'')g(x, z_0, \bar{r}') = g(x, z_0, \bar{r}'').$$

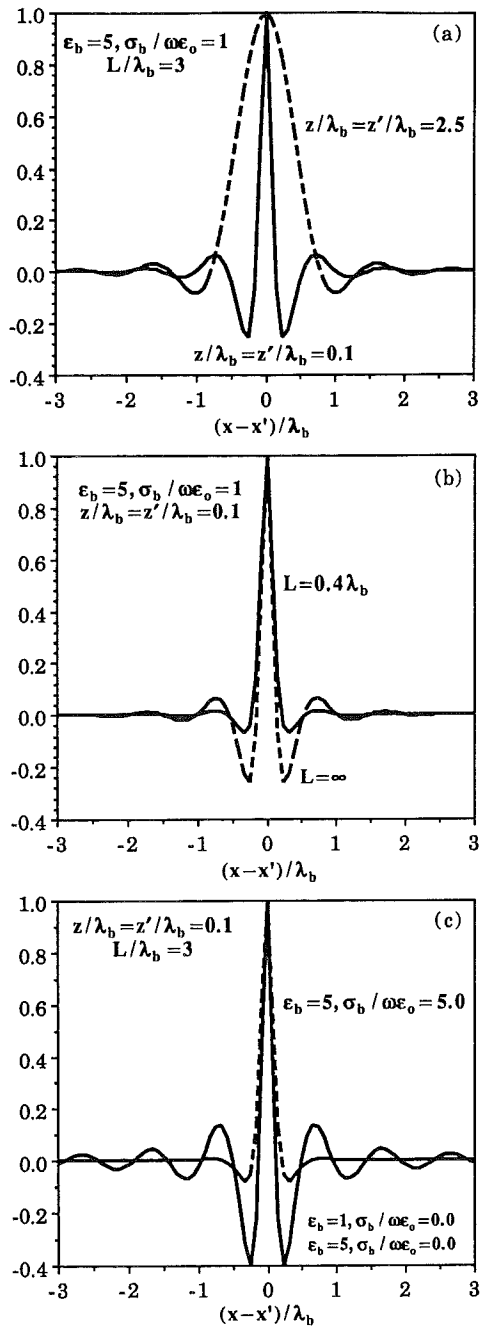

Figure A1. The induced current's resolution kernel as a function of distance along the x axis parallel to the measurement plane. (a) Varying observation point. (b) Varying slab thickness. (c) Varying background medium.

6. $\mathcal{R}(x-x', z', z')$ satisfies the following equality:

$$\int_0^L dz'\, \mathcal{R}(x-x', z', z') = \delta(x-x').$$

7. The nonradiating source $J_{NR}(\bar{r}, \bar{r}_n)$ belongs to the annihilator of the resolution kernel:

$$\int_0^L dz' \int_{-\infty}^{\infty} dx'\, \mathcal{R}(x-x', z, z') J_{NR}(\bar{r}', \bar{r}_n) = 0.$$

8. At zero frequency the resolution kernel is

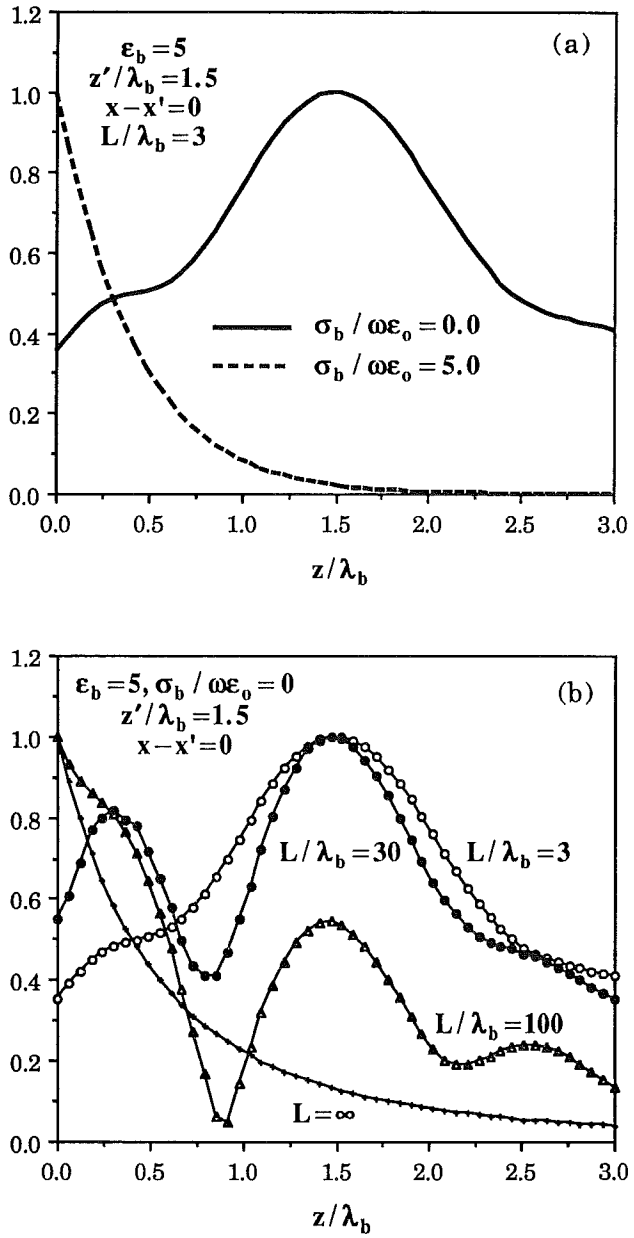

Figure A2. The induced current's resolution kernel as a function of distance along the z axis perpendicular to the measurement plane. (a) Varying conductivity of background medium. (b) Varying slab thickness.

$$\mathcal{R}(x-x', z, z') = \frac{2}{\pi}\sum_{n=0}^{\infty}\frac{(z+z'+2nL)^2-(x-x')^2}{[(z+z'+2nL)^2+(x-x')^2]^2}.$$

Equation (91) expresses the minimum norm solution as a weighted average or filtered version of the actual induced current. The filter is the resolution kernel. A perfect resolution kernel is a delta function in space; resulting in a minimum norm solution that is equal to the actual induced current. In many practical cases the minimum norm solution will be a smoothed or (spatially) low-passed filtered version of the actual induced currents.

Figure A1 shows the resolution kernel for the slab problem along the x axis parallel to the measurement plane. Figure A2 shows the resolution kernel along the z axis perpendicular to the measurement plane. The value of the kernel is normalized such that its maximum is unity. All dimensions are normalized with respect to the wavelength of the background medium.

Figure A1a shows that the resolution parallel to the plane of measurement degrades as we move away from the plane. Figure A1b shows that the resolution is independent on the thickness of the slab; however, for thicker slabs, contributions from points adjacent to the source point ($x = x'$) become larger as manifested in the appearance of side lobes. Figure A1c shows that the resolution parallel to the measurement plane is determined by the wavelength in the background medium, since the width of the curves are weakly dependent on the background's electrical parameters. As the medium becomes lossless, contributions from points adjacent to the source points become larger.

Figure A2a shows that the resolution perpendicular to the measurement plane is poorer than that parallel to the plane. It also shows that the resolution is lost as the medium becomes lossy. Figure A2b shows that as the slab thickness increases, the resolution degrades and is eventually lost for an infinite slab.

Appendix C: Positivity Constraints on the Reconstructed Electrical Susceptibility and Conductivity Structures

Positivity can be imposed on the reconstructed susceptibility $\chi(\bar{r}) = \varepsilon(\bar{r})/\varepsilon_0 - 1$ and conductivity $\sigma(\bar{r})$ by first recasting the constitutive relationship of (43) as follows [*Kohn and McKenney*, 1990]:

$$\sigma(\bar{r}) - i\omega\varepsilon_0\chi(\bar{r}) = \frac{j_s(\bar{r}, \bar{r}_n; \omega)}{E(\bar{r}, \bar{r}_n; \omega)}$$

$$= \frac{u(\bar{r}, \bar{r}_n; \omega) - iv(\bar{r}, \bar{r}_n; \omega)}{|E(\bar{r}, \bar{r}_n; \omega)|}, \tag{93}$$

where

$$j_s(\bar{r}, \bar{r}_n; \omega) = J_s(\bar{r}, \bar{r}_n; \omega) + [\sigma_b - i\omega(\varepsilon_b - \varepsilon_0)]E(\bar{r}, \bar{r}_n; \omega),$$

$$u(\bar{r}, \bar{r}_n; \omega) = \text{Re}\,\{j_s(\bar{r}, \bar{r}_n; \omega)E^*(\bar{r}, \bar{r}_n; \omega)\}/|E(\bar{r}, \bar{r}_n; \omega)|,$$

$$v(\bar{r}, \bar{r}_n; \omega) = -\text{Im}\,\{j_s(\bar{r}, \bar{r}_n; \omega)E^*(\bar{r}, \bar{r}_n; \omega)\}/|E(\bar{r}, \bar{r}_n; \omega)|.$$

Next, the cost function of (57) is split into two functions,

$$C_1'(\sigma) = \sum_{n,m}[\{\sigma(\bar{r})\}^{-1/2}u(\bar{r}, \bar{r}_n; \omega_m) - \{\sigma(\bar{r})\}^{1/2}|E(\bar{r}, \bar{r}_n; \omega_m)|]^2, \tag{94}$$

$$C_1''(\chi) = \sum_{n,m}[(\omega_m\varepsilon_0)^{-1/2}\{\chi(\bar{r})\}^{-1/2}v(\bar{r}, \bar{r}_n; \omega_m) - (\omega_m\varepsilon_0)^{1/2}\{\chi(\bar{r})\}^{1/2}|E(\bar{r}, \bar{r}_n; \omega_m)|]^2. \tag{95}$$

The differences between these new cost functions and the previous one (equation (57)) vanish at the true value of $Q(\bar{r}; \omega)$. The new cost functions are measures of the dissipated and stored powers, respectively. The values of $\sigma(\bar{r})$ and $\chi(\bar{r})$ that minimize these cost functions are

$$\sigma(\bar{r}) = \left(\sum_{n,m}\{u(\bar{r}, \bar{r}_n; \omega_m)\}^2\right)^{1/2}\left(\sum_{n,m}\left|E(\bar{r}, \bar{r}_n; \omega_m)\right|^2\right)^{-1/2}, \tag{96}$$

$$\chi(\bar{r}) = \frac{1}{\varepsilon_0}\left(\sum_{n,m}\frac{1}{\omega_m}\{v(\bar{r}, \bar{r}_n; \omega_m)\}^2\right)^{1/2} \cdot \left(\sum_{n,m}\omega_m\left|E(\bar{r}, \bar{r}_n; \omega_m)\right|^2\right)^{-1/2}. \tag{97}$$

Hence

$$Q(\bar{r};\omega)=\left[\left(\frac{\sum_{n,m}\{u(\bar{r},\bar{r}_n;\omega_m)\}^2}{\sum_{n,m}|E(\bar{r},\bar{r}_n;\omega_m)|^2}\right)^{1/2}-\sigma_b\right]$$
$$-i\omega\left[\left(\frac{\sum_{n,m}\{v(\bar{r},\bar{r}_n;\omega_m)\}^2/\omega_m}{\sum_{n,m}\omega_m|E(\bar{r},\bar{r}_n;\omega_m)|^2}\right)^{1/2}+\varepsilon_0-\varepsilon_b\right]. \quad (98)$$

Acknowledgments. We would like to thank Carlos Torres-Verdin, Vladimir Druskin, and Apo Sezginer for their valuable feedback.

References

Aki, K., and P. G. Richards, *Quantitative Seismology: Theory and Methods*, W. H. Freeman, New York, 1980.

Bleistein, N., and J. K. Cohen, Nonuniqueness in the inverse source problem in acoustics and electromagnetics, *J. Math. Phys. N.Y.*, *18*, 194–201, 1977.

Bolomey, J. C., C. Pichot, and G. Garboriaud, Planar microwave imaging camera for biomedical applications: Critical and prospective analysis of reconstruction algorithms, *Radio Sci.*, *26*, 541–549, 1991.

Caorsi, S., G. L. Gragnani, and M. Pastorino, Two-dimensional microwave imaging by a numerical inverse scattering solution, *IEEE Trans. Microwave Theory Tech.*, *38*, 981–989, 1990.

Caorsi, S., G. L. Gragnani, and M. Pastorino, A multiview microwave imaging system for two-dimensional penetrable objects, *IEEE Trans. Microwave Theory Tech.*, *39*, 845–851, 1991.

Caorsi, S., G. L. Gragnani, and M. Pastorino, Numerical solution to three-dimensional inverse scattering for dielectric reconstruction purposes, *IEE Proc. H*, *139*, 45–52, 1992.

Cavicchi, T. J., S. A. Johnson, and W. D. O'Brien, Application of the sinc basis moment method to the reconstruction of infinite circular cylinders, *IEEE Trans. Ultrason. Ferroelectr. Freq. Control.*, *35*, 22–33, 1988.

Conte, S. D., and C. de Boor, *Elementary Numerical Analysis: An Algorithmic Approach*, McGraw-Hill, New York, 1980.

Devaney, A. J., and G. C. Sherman, Nonuniqueness in inverse source and scattering problems, *IEEE Trans. Antennas Propag.*, *AP-30*, 1034–1037, 1982.

Devaney, A. J., and E. Wolf, Radiating and nonradiating classical current distributions and the fields they generate, *Phys. Rev. D Part. Fields*, *8*, 1044–1047, 1973.

Gamliel, A., K. Kim, A. I. Nachman, and E. Wolf, A new method for specifying nonradiating, monochromatic scalar sources and their fields, *J. Opt. Soc. Am. A Opt. Image Sci.*, *6*, 1388–1393, 1989.

Habashy, T. M., and D. G. Dudley, Inversion of permittivity and conductivity using the renormalized source-type integral equation approach: A review, paper presented at Progress in Electromagnetic Research Symposium, Mass. Inst. of Technol., Cambridge, Mass., July 1989a.

Habashy, T. M., and D. G. Dudley, Simultaneous inversion of permittivity and conductivity profiles using a renormalized source-type integral equation approach, paper presented at URSI International Symposium on Electromagnetic Theory, Int. Union of Radio Sci., Stockholm, Sweden, August 1989b.

Habashy, T. M., and R. Mittra, On some inverse methods in electromagnetics, *J. Electromagn. Waves Appl.*, *1*, 25–58, 1987.

Habashy, T. M., E. Y. Chow, and D. G. Dudley, Profile inversion using the renormalized source-type integral equation approach, *IEEE Trans. Antennas Propag.*, *AP-38*, 668–682, 1990.

Habashy, T. M., M. L. Oristaglio, and A. T. de Hoop, Simultaneous inversion of permittivity and conductivity structures employing a nonperturbative approach, *Proc. SPIE Int. Soc. Opt. Eng.*, 1767, 193–207, 1992.

Johnson, S. A., and M. L. Tracy, Inverse scattering solutions by a sinc basis, multiple source, moment method, 1, Theory, *Ultrason. Imaging*, *5*, 361–375, 1983.

Johnson, S. A., Y. Zhou, M. L. Tracy, M. J. Berggren, and F. Stenger, Inverse scattering solutions by a sinc basis, multiple source, moment method, 3, Fast algorithms, *Ultrason. Imaging*, *6*, 103–116, 1984.

Kleinman, R. E., and P. M. van den Berg, Profile inversion via successive over-relaxation, *Proc. SPIE Int. Soc. Opt. Eng.*, 1351, 129–139, 1990a.

Kleinman, R. E., and P. M. van den Berg, Nonlinearized approach to profile inversion, *Int. J. Imaging Syst. Technol.*, *2*, 119–126, 1990b.

Kohn, R. V., and A. McKenney, Numerical implementation of a variational method for electrical impedance tomography, *Proc. SPIE Int. Soc. Opt. Eng.*, *6*, 389–414, 1990.

Kong, J. A., *Electromagnetic Wave Theory*, John Wiley, New York, 1986.

Ney, M. M., A. M. Smith, and S. S. Stuchly, A solution of electromagnetic imaging using pseudoinverse transformation, *IEEE Trans. Med. Imaging*, *MI-3*, 155–162, 1984.

Tracy, M. L., and S. A. Johnson, Inverse scattering solutions by a sinc basis, multiple source, moment method, 2, Numerical evaluation, *Ultrason. Imaging*, *5*, 376–392, 1983.

A. T. de Hoop, Delft University of Technology, Department of Electrical Engineering, P.O. Box 5031, 2600 GA Delft, Netherlands.

T. M. Habashy and M. L. Oristaglio, Schlumberger-Doll Research, Old Quarry Road, Ridgefield, CT 06877-4108.

(Received October 7, 1992; revised May 29, 1993; accepted May 29, 1993.)